ELSEVIER

Biophysical Chemistry 58 (1996) 225–237

Biophysical Chemistry

Correlated motions and propagation of the effect of a local conformational change in the transmembrane helix of the c-*erb*B2 encoded protein and in its V659E mutant, studied by molecular dynamics simulations

Norbert Garnier [a,b,*], Daniel Genest [a], Monique Genest [a]

[a] *Centre de Biophysique Moléculaire, CNRS, Rue Charles Sadron, 45071 Orleans Cedex 2, France*
[b] *Université d'Orléans, Rue Charles Sadron, 45071 Orleans Cedex 2, France*

Received 21 November 1994; revised 19 May 1995; accepted 26 June 1995

Abstract

A detailed study of the dynamical behavior of the 29-residue peptide including the transmembrane domain of p185$^{c\text{-}erbB2}$ oncogene-encoded protein and of its V659E mutant is presented. In a first part of this work we analyse equal time correlation coefficients between the backbone dihedral angle fluctuations. Concerted motions are observed in the wild type transmembrane α-helix but not in the corresponding V659E intramembrane domain. The difference observed in the correlation pattern is attributed to the single amino acid replacement.

In a second part, we investigate the propagation of the effect of a local conformational change along the transmembrane segment, one of the dominant hypotheses for signal transduction mechanisms of transmembrane receptors. The analysis of angular time correlation functions together with that of the response of the different residues to a local disturbance applied at the N-terminal side evidences a propagation phenomenon for the wild type peptide. This effect is much less clear for the mutated peptide. Furthermore we show that the first one is much more flexible than the second one.

Keywords: Molecular dynamics simulations; Transmembrane helix; c-*erb*B2 protein; Correlated motions; Signal propagation

1. Introduction

Dynamical aspects of biological molecules are of major importance for interpreting their structure and their function [1]. The motions in protein molecules may allow ligand binding or transmission of information such as local conformational change affecting the reactivity of a remote site. Moreover, specific residues or subunit displacements may have a significant role in the transition from inactive to active configurations of proteins and their internal motions can be affected by local alterations such as single amino acid replacement. Even fast, atomic or dihedral fluctuations in the femtosecond and picosecond time range may contribute to the occurrence of slow conformational changes [2].

* Corresponding author. Tel.: (33) 38517668; fax: (33) 38631517; e-mail: garnier@cnrs-orleans.fr.

SSDI 0301-4622(95)00106-9

Internal dynamics of biological molecules simulated using molecular dynamics techniques [1] is usually probed by average values, root mean square (rms) and time-series of dihedral angles and coordinates. However, these quantities give only a partial description of the internal dynamics of the biomolecule, and do not give information in particular about concerted motions of atoms. More complete information can be obtained from the analysis of equal time correlation coefficients and time correlation functions between the different atomic coordinates or dihedral angle fluctuations [3,4].

Recently [5], as an approach for investigating signal transduction mechanisms, we have applied molecular dynamics simulations on the transmembrane sequence of the c-*erb*B2 protein, a tyrosine kinase protein known as a member of the epidermal growth factor receptor (EGFR) family [6,7]. We have shown differences in the dynamical behavior between the wild transmembrane portion of $p185^{c\text{-}erbB2}$ and its V659E mutant. The differences originate from conformational transitions observed for the wild type peptide at the level of the mutation Val^{659} and a few residues far apart in the sequence.

In order to complement our first analysis [5], we are interested in the study of correlated motions in the helices. This study is presented in the first part of this paper where we report an analysis of the equal time correlation coefficients between the different dihedral angle fluctuations of the backbone for the two transmembrane segments. The existence of different correlation patterns for the wild and mutated transmembrane segments is evidenced.

A very important point investigated in this paper is directly related to signal transduction mechanisms. Two dominant mechanisms have been suggested to explain the signal transmission phenomenon across the membranes. One of these mechanisms which corresponds to an intramolecular process involves the propagation, along the intramembrane sequence, of a conformational change induced by ligand binding [8,9]. The second one, an intermolecular process, relies on the dimerization or oligomerization [6] of an active conformation of the transmembrane domain. It seems likely that these two mechanisms may coexist or may be cooperative and that dimerization or oligomerization is a consequence of internal fluctuations in the transmembrane part of the protein. The result of signal transduction is to induce important biological events such as proliferation or uncontrolled transformation of cells.

In the second part of this work, we focus on the first mechanism based on the hypothesis of a conformational perturbation propagation along the transmembrane sequence. Two different analyses, applied to both the wild type and mutated transmembrane segments are reported. One deals with the angular time correlation functions of the backbone dihedral angle fluctuations: this approach is justified by the dissipation fluctuations theorem [10] which states that a relationship exists between the response of a system to an external disturbance and the internal fluctuations at equilibrium. The second one, concerns the response of both peptides to a conformational change imposed at $t = 0$ at the level of the membrane interface. This is achieved by performing a series of short MD simulations. Both methods clearly show the propagation of a conformational perturbation along the wild type sequence. On the contrary, for the mutated sequence, the effect of the perturbation is very damped a few residues after the external disturbance location.

2. Methods

2.1. Long time MD simulations

Molecular dynamics simulations, used for correlation analysis, have been performed on two peptides including 22 residues of the transmembrane portion of the wild type and of the mutated V659E $p185^{c\text{-}erbB2}$ protein [5] to which three extracellular residues at the N-terminal and four intracellular residues at the C-terminal have been added. Each extremity has been capped by CH_3CO and $NHCH_3$ end groups, respectively.

The wild type sequence is as follows:–Leu^{1}–Thr–Ser–Ile^{4}–Ile–Ser–Ala–Val–Val^{9}–Gly–Ile–Leu–Leu–Val–Val–Val^{16}–Leu–Gly–Val–Val–Phe–Gly–Ile–Leu–Ile^{25}–Lys–Arg–Arg–Gln^{29} [7]. The mutated sequence is obtained by replacing Val^{9} by Glu^{9} in the protonated state, corresponding to the replacement of Val^{659} by Glu^{659} in the whole protein.

Both peptides were initially built as regular right-

handed α-helices with the conventional Φ and Ψ dihedral angles set to the values $-57°$ and $-47°$, respectively. Details of the MD protocol used to produce atomic trajectories are given elsewhere [5]. In vacuo simulations were performed using a united atom representation except for polar hydrogens. All bond lengths were kept constant by applying the SHAKE algorithm [11,12]. Each trajectory covers a period of 160 ps after equilibration at 300 K and coordinates are stored every 0.04 ps. For MD simulations, the GROMOS program [13] was used and all calculations were performed on a Crimson Silicon Graphics workstation. The obtention of the whole trajectory needs about 100 h of CPU time for each peptide.

2.2. Equal time correlation matrix

To quantify the dynamical behavior of both helices and in particular to identify concerted atomic motions, we have calculated the correlation matrix for the backbone dihedral angle fluctuations [14,15]. The correlation coefficient between two dihedral angles α_i and α_j fluctuations (with α referring either to Φ or Ψ dihedral angles of residue i and j, respectively) is defined by the expression:

$$C(\alpha_i,\alpha_j) = \frac{\langle \Delta\alpha_i \Delta\alpha_j \rangle}{\langle \Delta\alpha_i^2 \rangle^{\frac{1}{2}} \langle \Delta\alpha_j^2 \rangle^{\frac{1}{2}}} \quad (1)$$

where $\Delta\alpha_i = \alpha_i - \langle \alpha_i \rangle$ is the instantaneous deviation of α_i from its mean value $\langle \alpha_i \rangle$. The angle brackets represent an average over the whole trajectory and $\langle \Delta\alpha_i^2 \rangle$ is the mean square dihedral angle fluctuations. Diagonal elements ($i = j$) of the correlation matrix are equal to 1 and for $i \neq j$ the dihedral angle fluctuations are correlated when $C(\alpha_i,\alpha_j) > 0$ or anti-correlated when $C(\alpha_i,\alpha_j) < 0$. Obviously, the equal time correlation matrix is symmetrical.

This type of correlation matrix has been recently used for the study of atomic displacements in HIV-I protease dimer [16] and in BPTI (bovine pancreatic trypsin inhibitor) [17].

2.3. Time dependence of the correlation matrix

Each coefficient of the correlation matrix defined by Eq. 1 expresses the dependence of the value taken by a quantity $\Delta\alpha_i$ at a given time with the value taken by another quantity $\Delta\alpha_j$ at the same time. This coefficient does not indicate the duration of the correlation, i.e. the dependence between the value taken by $\Delta\alpha_j$ at a given time and the value taken by $\Delta\alpha_i$ at an earlier time. Such information is obtained from the time correlation functions defined by:

$$C(\alpha_i,\alpha_j)(m\tau) = \frac{\frac{1}{(N-m)} \sum_{n=1}^{N-m} \Delta\alpha_i(n\tau)\Delta\alpha_j((n+m)\tau)}{\left(\frac{1}{(N-m)} \sum_{n=1}^{N-m} \Delta\alpha_i^2(n\tau)\right)^{\frac{1}{2}} \left(\frac{1}{(N-m)} \sum_{n=1}^{N-m} \Delta\alpha_j^2((n+m)\tau)\right)^{\frac{1}{2}}} \quad (2)$$

where τ is the time interval used for coordinate storage (0.04 ps), $m\tau$ is the delay time (m varies from 0 to 500 in our study). n labels the various stored configurations the total number of which is N (4000 in this work). The correlation functions are therefore calculated over 20 ps. The whole set of $C(\alpha_i,\alpha_j)(m\tau)$ for a given value of m constitutes a time dependent correlation matrix which is not symmetrical. We note that for $m = 0$ Eq. 2 reduces to Eq. 1. The time dependent correlation matrix has been established for both transmembrane peptides.

2.4. Short MD simulations: local perturbation propagation

Starting from an equilibrium structure and a set of atomic velocities, two short MD simulations of 2 ps are performed, one at equilibrium (without any external perturbation) and one out of equilibrium by forcing a structural deformation at residue Ile^4 at time $t = 0$ maintained up to the end of the simulation. This perturbation is applied by imposing arbitrarily $\Psi_4 = 90°$, which corresponds to an allowed conformation defined in the Ramachandran map and results in a kink of the helical structure. The Ψ_4 value is constrained by using a harmonic potential with a force constant equal to 500 kJ mol^{-1} deg^{-2}. The equilibrium structure is taken as the last conformation obtained at the end of the previous 160 ps MD simulations [5], and initial velocities are randomly extracted from a Maxwell distribution centered at 300 K. The simulations are carried out using

GROMOS [13] with a time step of 0.002 ps and all bond lengths are kept constant with the SHAKE algorithm [11,12]. Atomic coordinates are stored every 0.004 ps and therefore each MD simulation contains 500 configurations.

This procedure is repeated $L = 20$ times, starting from different initial conditions for velocities but with the same initial structure. The mean difference between the values of each backbone dihedral angle measured at equilibrium and out of equilibrium is calculated as a function of time using the following expression:

$$\langle \alpha_i^{NP}(t) - \alpha_i^{P}(t) \rangle = \frac{1}{L} \sum_{k=1}^{L} \left(\alpha_{i,k}^{NP}(t) - \alpha_{i,k}^{P}(t) \right) \tag{3}$$

with α_i denoting either the Φ_i or Ψ_i dihedral angles of residue i and $t = n \times 0.004$ ps ($n = 1,...500$). The index k specifies the different simulations. Subscripts NP and P characterize quantities calculated from the trajectory obtained from the no perturbed helix simulations (Ψ_4 not constrained) and the perturbed helix simulations (Ψ_4 constrained), respectively.

This study was carried out for both peptides. The MD simulations needed about 100 h of CPU time and 250 MBytes of file storage.

3. Results

3.1. Equal time correlation

In this section, we present the results of the study of the correlation coefficients between the Φ and Ψ dihedral angle fluctuations for both transmembrane helices. The analysis was carried out on the 160 ps trajectories obtained for each α-helix, one with the wild type sequence and the second one with the mutated Glu^9 sequence.

The equal time correlation coefficients $C(\alpha_i, \alpha_j)$ are calculated between the whole set of Φ and Ψ dihedral angle fluctuations for residues 2 to 29 using Eq. 1. The correlation maps for the wild type helix and the mutated helix are shown in Fig. 1. For clarity, only the correlation coefficients with absolute values greater than 0.20 are shown. This value deter-

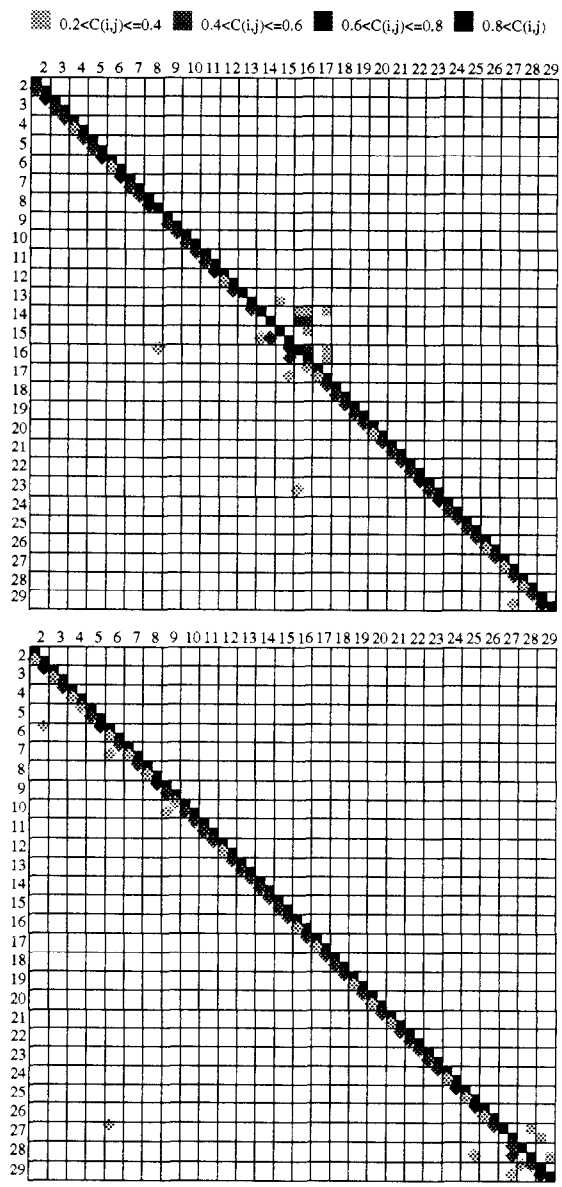

Fig. 1. Equal time correlation maps (top: wild type sequence; bottom: Glu^{659} mutated sequence). Correlations are calculated between the Φ and Ψ dihedral angle fluctuations of residues numbered 2 to 29 (see text). Correlations coefficients greater than 0.20 in absolute value are represented by a symbol proportionally shaded with the degree of correlation. Each grid cell ij contains the correlations between the Φ and Ψ dihedral angle fluctuations of residues i and j. Positive correlations (square) are collected in the upper diagonal part of the map and negative correlations (diamond) are collected in the lower diagonal part of the map.

mines the threshold under which variables are considered uncorrelated. Four classes specifying the degree of correlation are introduced: the two first classes define weak correlations for $|C(\alpha_i,\alpha_j)| < 0.40$ and moderate correlations for $0.4 < |C(\alpha_i,\alpha_j| < 0.6$, the two last classes define strong correlations for $0.6 < |C(\alpha_i,\alpha_j)| < 0.8$ and very strong correlations for $0.8 < |C(\alpha_i,\alpha_j)|$. In Fig. 1, each grid cell of a correlation map represents the correlation coefficients between the Φ and Ψ fluctuations of residues i and j, respectively. The symbol characterizing one coefficient is shaded according to the class of the correlation. The symmetry of the correlation matrix allows to gather correlations and anti-correlations in the upper part of the diagonal (positive coefficients) and in the lower part of the diagonal (negative coefficients), respectively. Diagonal elements corresponding to the auto-correlations $C(\Phi_i, \Phi_i)$ and $C(\Psi_i\ \Psi_i)$ are also represented. Obviously, they are all equal to 1.

Examination of the correlation map of the dihedral angle fluctuations of the wild type α helix (Fig. 1 top) reveals concerted rotations between nearest neighbors. Most of the fluctuations of the dihedral angle pairs (Φ_i, Ψ_i) and (Ψ_i, Φ_{i+1}) are moderately anti-correlated. However, the anti-correlation pattern is broken and lacks of correlated motions are found in two regions: (1) at the (Ψ_8, Φ_9) level and (2) in the zone ranging from Φ_{13} to Ψ_{16}. No correlation or anti-correlation is observed for the pairs (Φ_{13}, Ψ_{13}), (Φ_{14}, Ψ_{14}), (Ψ_{14}, Φ_{15}) and (Φ_{15}, Ψ_{15}). On the contrary, a moderate positive correlation is found for (Φ_{16}, Ψ_{16}). We point out that these two regions coincide with the two flexible zones discussed in a previous work [5].

In addition, in the central part of the helix, from residue Leu^{13} to residue Leu^{17}, several concerted motions are observed between non-adjacent dihedral angle fluctuations. For example, fluctuations of Ψ_{16} are correlated to those of Ψ_{17}, Φ_{15}, Φ_{14} and Ψ_{14} while they are anti-correlated to those of Ψ_{15}. It is also important to note that both flexible regions of the helix are related by an anti-correlation between Ψ_8 and Φ_{16} fluctuations. An other anti-correlation is found between Φ_{16} and Ψ_{23} fluctuations. We remark that the two residues Val^8 and Val^{16} and two other residues namely Val^{16} and Ile^{23} are separated by about two helix turns.

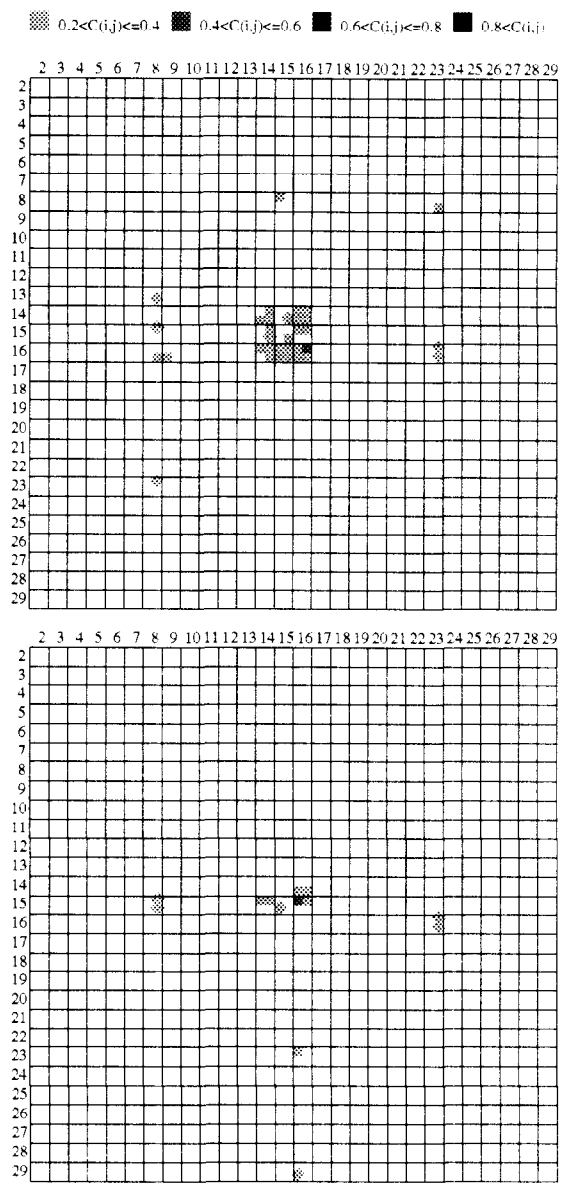

Fig. 2. Delayed correlations between the backbone Φ and Ψ dihedral angle fluctuations of the wild type helix. Correlation coefficients greater than 0.20 in absolute value are represented by a symbol proportionally shaded with the degree of the correlation. For a row i and a column j, each element of the maps is defined by $C(\alpha_i,\alpha_j)(t)$ for positive correlations (square) and $C(\alpha_j,\alpha_i)(t)$ for negative correlations (diamond) with $\alpha = \Phi$ or Ψ and $t = 10$ ps (top) or 20 ps (bottom).

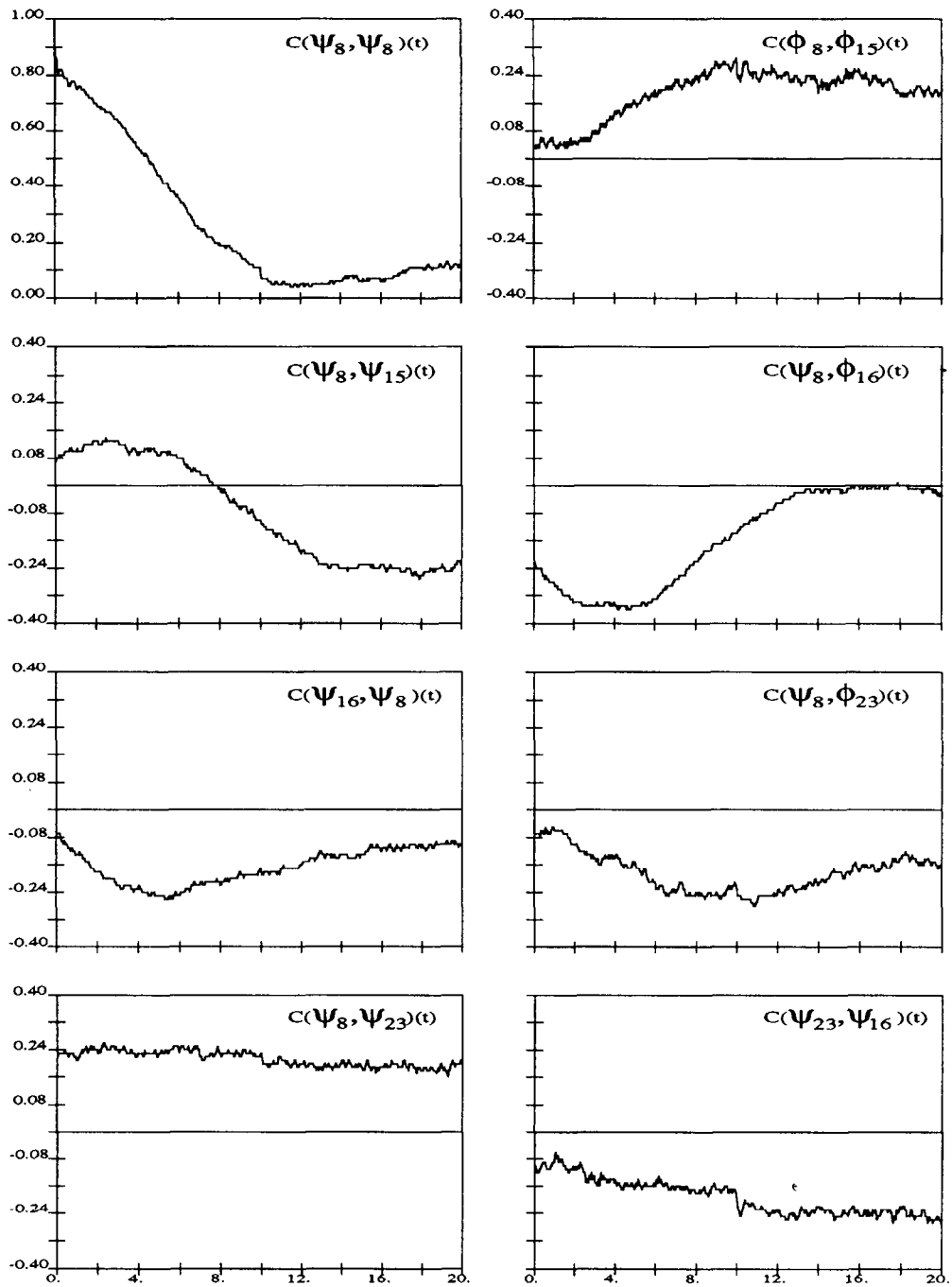

Fig. 3. Examples of time correlation functions between backbone Φ, Ψ dihedral angle fluctuations of the wild type helix. Time is given in ps.

along the sequence one observes anti-correlations between nearest neighbors except for two pairs at the C-terminal part of the helix. At the mutation point, the strong anti-correlation between Ψ_8 and Φ_9 fluctuations ($C(\Psi_8, \Phi_9) = -0.62$) is ten-fold higher than that found for the wild type sequence.

Correlations and anti-correlations between non-adjacent angle fluctuations are observed only at the C-terminal part of the helix which is not included in the intramembrane part of the peptide. Anti-correlations occur for the three pairs of dihedral angles (Φ_6, Ψ_2), (Φ_6, Ψ_7) and (Φ_9, Ψ_{10}) but not in the central part of the helix. The only anti-correlation involving residues located at long distance is observed between Φ of residue Ser^6 and Ψ of residue Arg^{27}, a C-terminal residue.

3.2. Time dependent correlation functions

3.2.1. Wild peptide

The correlations between angular fluctuations at time $t = 0$ and angular fluctuations after 10 ps and 20 ps are illustrated in Fig. 2. A first observation concerns the disappearance of most of the diagonal elements of the correlation matrix after a delay of 10 ps, except for residues Val^{14}, Val^{15} and Val^{16} (Fig. 2 top). This result strongly suggests a fast relaxation process between adjacent neighbors.

A second observation concerns the correlations between nearest neighbors which also vanish except in the central part of the helix. At the opposite, long time correlations exist between the three zones defined by the groups of residues Val^8–Val^9, Leu^{13}–Val^{16} and Ile^{23}. The correlation pattern between these three zones becomes more populated after a delay of 10 ps compared to that observed at equal time (see Fig. 1 top). For example, concerted motions between Val^8 and Ile^{23} are seen after 10 ps but are absent or too low, under the threshold, to be detected in the equal time correlation matrix. These long range concerted motions are expressed by correlations between the fluctuations of Ψ_8 and Ψ_{23} and anti-correlations between those of Ψ_8 and Φ_{23}. Several other correlation or anti-correlation peaks appear, even after a delay of 20 ps such as the pair (Ψ_8, Ψ_{15}), or are amplified such as the pair (Φ_{15}, Φ_{16}) (Fig. 2 bottom). For this last pair, no correlation was observed at equal time, but after a delay of 10 ps, Φ_{15} and Φ_{16} fluctuations become weakly correlated and 20 ps latter they become moderately correlated with a correlation coefficient two times higher. These delayed correlations suggest a propagation process.

More details on the time dependence of correlation are contained in the correlation functions. Some examples are given in Fig. 3 and as shown for most of the curves, the absolute value of $C(\alpha_i, \alpha_j)(t)$ increases after a few picoseconds. An example is the

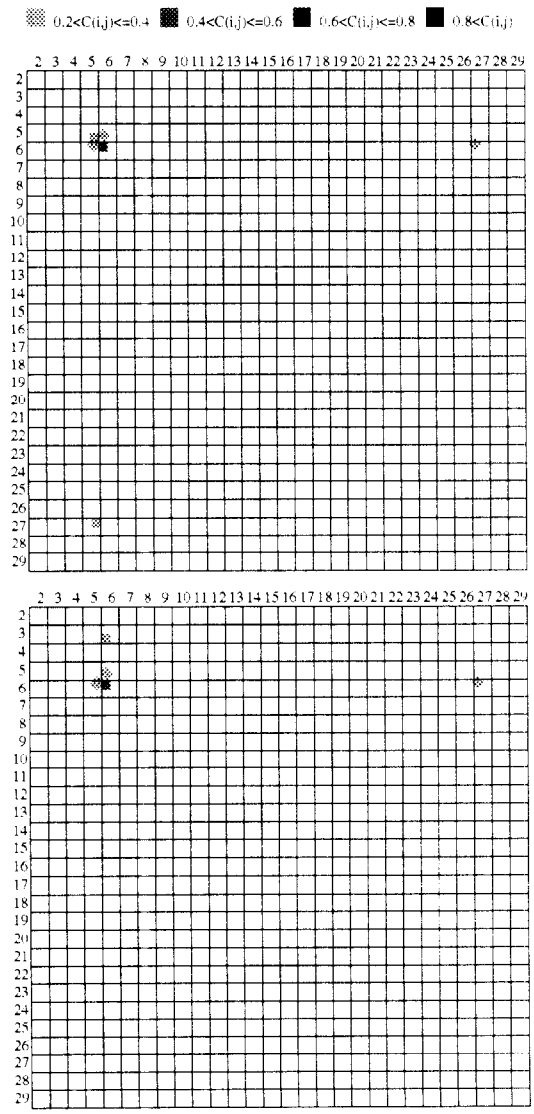

Fig. 4. Delayed correlations between the backbone Φ and Ψ dihedral angle fluctuations of the Glu^{659} mutated helix. Same conditions as in Fig. 2.

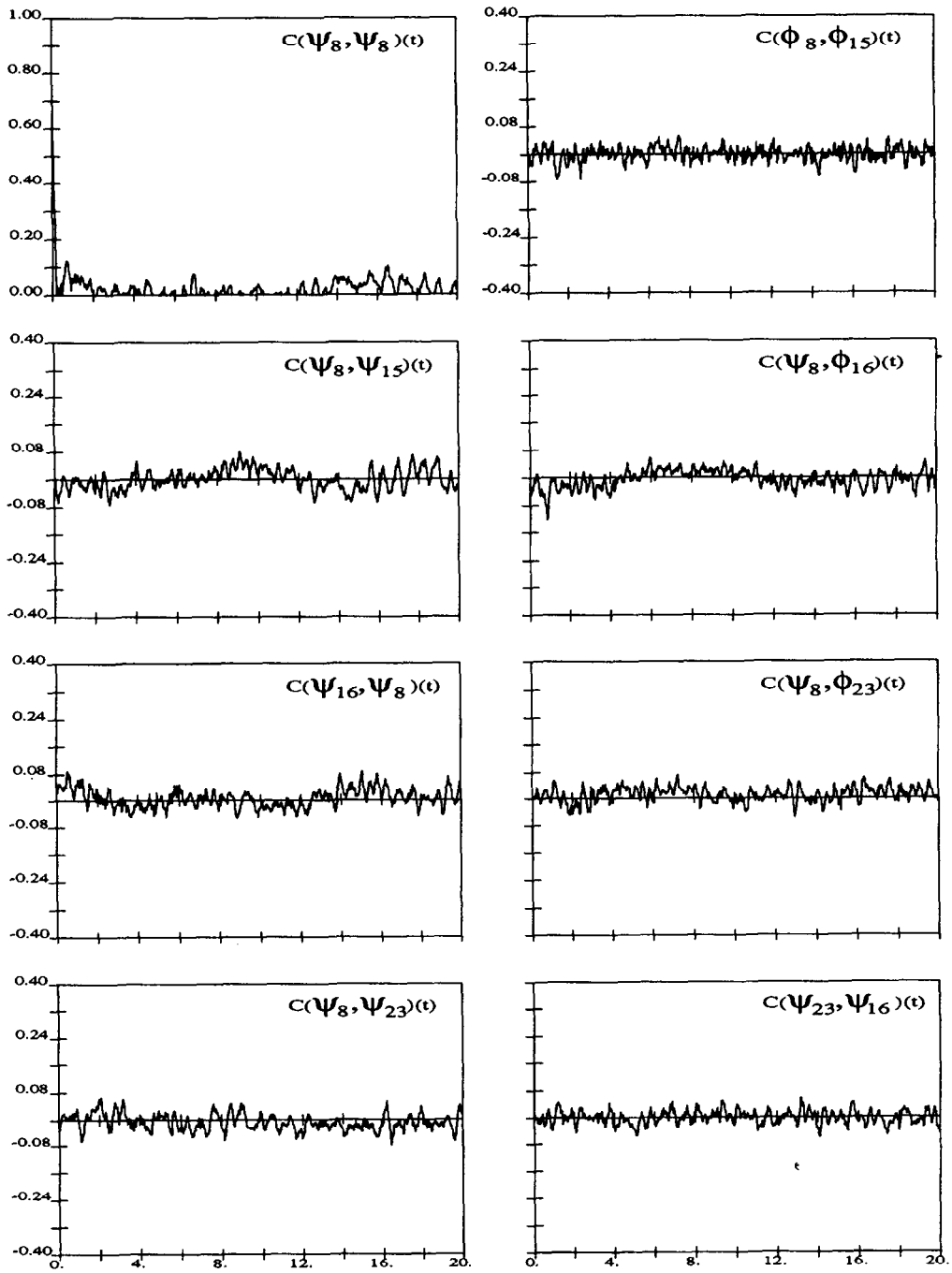

Fig. 5. Examples of time correlation functions between backbone Φ, Ψ dihedral angle fluctuations of the Glu^{659} mutated helix. Time is given in ps.

auto-correlation function $C(\Psi_8, \Psi_8)(t)$ which decreases very fast after a few picoseconds and reaches a low value after 10 ps. The correlation between $\Phi_8(O)$ and $\Phi_{15}(t)$ fluctuations, two angles pertaining to distant residues, appears after a short time of 3 ps and increases up to 0.24 after 10 ps. Also, the anti-correlation observed between the $\Psi_8(0)$ fluctuations and those of $\Phi_{16}(t)$ completely disappears after 12 ps. Motions weakly correlated at a short time may become anti-correlated after a longer delay as for $C(\Psi_8, \Psi_{15})(t)$. All these examples clearly demonstrate the existence of a propagation process throughout the wild peptide.

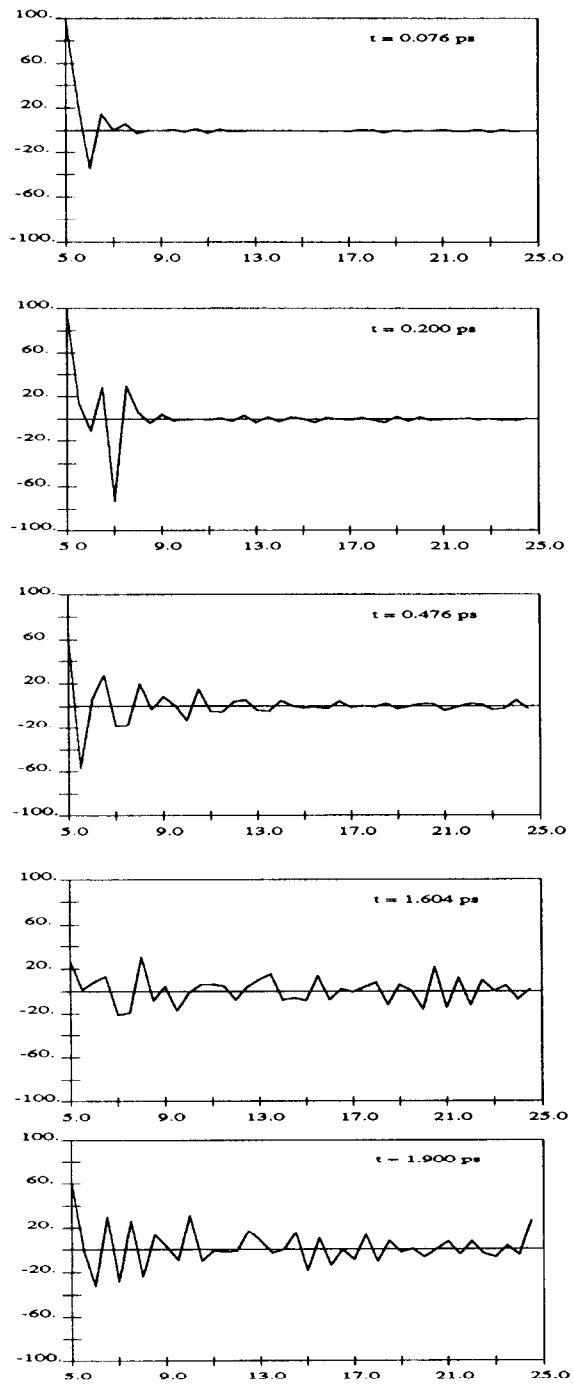

3.2.2. Mutated peptide

Fig. 4 shows the correlation between angular fluctuations for the mutated peptide after 10 ps and 20 ps. As for the wild peptide, one observes the disappearance of the diagonal elements except for residues Ile^5 and Ser^6. The long time correlation pattern is much less populated than for the wild peptide. The only long distance correlations are for Φ_6, Φ_{27} and Ψ_5, Φ_{27}. Therefore, there is no evidence of a propagation process. The above considerations are confirmed by the time dependent correlation functions (Fig. 5). All the cross-correlation functions fluctuate around the value zero demonstrating that any backbone dihedral angle moves independently of the other one. Furthermore, auto-correlation functions such as $C(\Psi_8, \Psi_8)(t)$ (left top in Fig. 5), shows that the fluctuations of a given angle become quickly uncorrelated. All these observations show that there is no time dependence and thus do not evidence a propagation process.

3.3. Propagation of a conformational change

3.3.1. Wild peptide

The differences between the perturbed and the unperturbed dynamics of the wild type transmembrane helix have been followed during 2 ps. Results are shown in Fig. 6 which gives the mean value of

Fig. 6. Average difference between backbone dihedral angles obtained from the perturbed and unperturbed MD simulations of the wild type helix at different times (see text). The mean differences $\langle \Phi_i^{NP} - \Phi_i^{P} \rangle$ and $\langle \Psi_i^{NP} - \Psi_i^{P} \rangle$ (ordinate in degrees) calculated from two sets of 20 MD simulations of 2 ps each, are given sequentially for each residue numbered from Ile^5 to Leu^{24} (abscissa).

the backbone dihedral angle differences at five different times. For each plot, the mean differences $\langle \Phi_i^{NP} - \Phi_i^{P} \rangle$ and $\langle \Psi_i^{NP} - \Psi_i^{P} \rangle$ are reported for each residue i specified in the abscissa.

At a short time interval ($t = 0.076$ ps), the plot reveals that only the two nearest residues Ile[5] and Ser[6] are affected by the perturbation. Their dihedral angle variations are 100° for Φ_5 but only 20° for Ψ_5 and −35° and +20° for Φ_6 and Ψ_6, respectively. These large deviations are associated with an important atomic rearrangement essential for optimizing the new interactions generated by the deformation imposed at the Ile[4] residue. At $t = 0.200$ ps, the Ψ_4 perturbation is propagated up to residue Ala[7] for which the observed differences are about −70° for

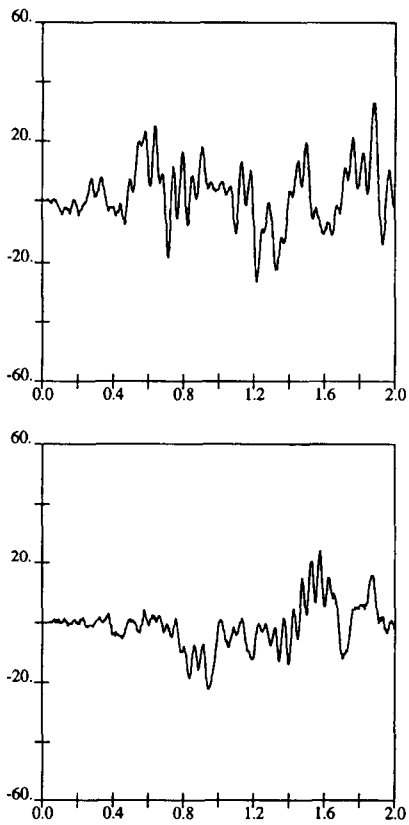

Fig. 7. Time series of the $\langle \Psi_8^{NP} - \Psi_8^{P} \rangle$ (top) and $\langle \Psi_{23}^{NP} - \Psi_{23}^{P} \rangle$ (bottom) of the wild type helix. Time is given in ps, and angles in degrees. Same conditions as in Fig. 6.

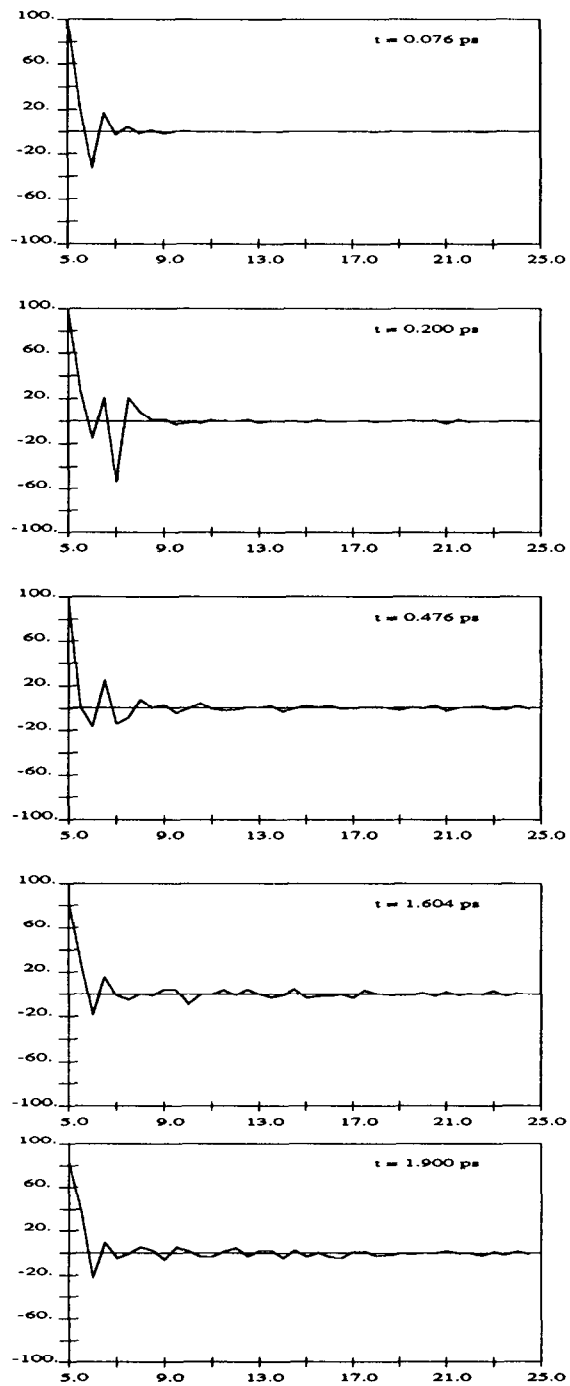

Fig. 8. Average difference between backbone dihedral angles obtained from the perturbed and unperturbed MD simulations of the Glu[659] mutated helix at different times (see text). Same conditions as in Fig. 6.

Φ_7 and 20° for Ψ_7 leading to an important structural change of the perturbed helix at this position.

The propagation process is clearly displayed at $t = 0.476$ ps and the deformation of the helical structure from residues Ile^5 to Gly^{10} is observed with different magnitude effects. More latter, at 1.604 ps, all the residues of the sequence are affected by the kink imposed at the beginning of the helix. A striking feature is the Φ_8 dihedral angle deviation still relatively large, characterized by a value equal to 30°. The largest deviations are observed for Ψ_{13}, Ψ_{15}, Ψ_{18}, Φ_{20}, Ψ_{20} and Φ_{21} dihedral angles. Finally, at $t = 1.900$ ps, all the residues are still affected.

Fig. 7 shows examples of time series of the deviations calculated for Ψ_8 (top) and Ψ_{23} (bottom).

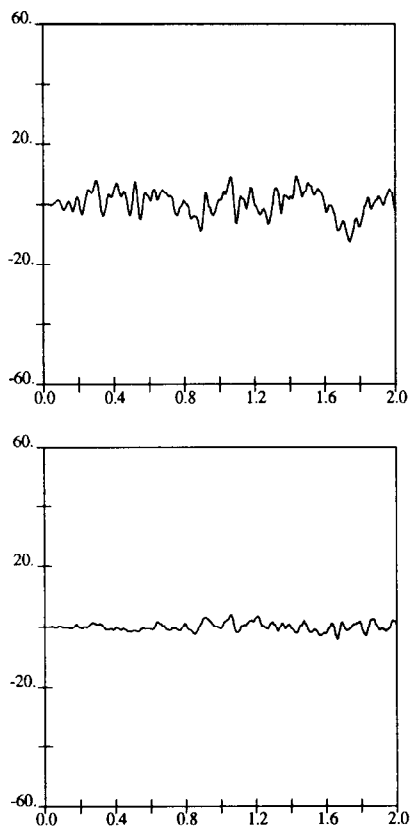

Fig. 9. Time series of the $\langle \Psi_8^{NP} - \Psi_8^{P} \rangle$ (top) and $\langle \Psi_{23}^{NP} - \Psi_{23}^{P} \rangle$ (bottom) of the Glu^{659} mutated helix. Time is given in ps, and angles in degrees. Same conditions as in Fig. 6.

It is clear that the response to the perturbation is detected after a delay longer for residue Ile^{23} than for residue Val^8. This observation is a direct evidence of the propagation phenomenon.

3.3.2. Mutated peptide

Fig. 8 shows the response of the backbone dihedral angles Φ, Ψ to the disturbance, at different times. The major observation is that most of the residues are weakly perturbed, even after 1.9 ps. The effect of the initial perturbation remains localized at the N-terminal part of the peptide and the propagation of the disturbance seems to be strongly damped after residues Glu^9–Gly^{10}. A propagation process is, however, observed up to the C-terminal end of the transmembrane segment, but it consists of very weak perturbations of the dihedral angles. This is also observed in Fig. 9 exhibiting much less important perturbations than for the wild peptide. These observations hold for any dihedral angle of the backbone.

4. Discussion and conclusion

We present a detailed analysis of the internal motions of two peptides including the transmembrane domains of the c-*erb*B2 proto-oncogene protein and of the oncogenic V659E form. This study is based on molecular dynamics simulations performed in vacuo [5]. This approximation does not seem inappropriate to approach the study of motions in transmembrane peptides. Indeed, a relative dielectric constant of 1 is used in all the simulations and this value is very close to that given in membrane environment [$\epsilon = (2\text{–}4)\epsilon_0$] [18], contrarily to that of water which is much higher [$\epsilon = 80\epsilon_0$]. Besides, the electrostatic interactions between a highly hydrophobic sequence and the apolar environment are low. Consequently, the interactions between the helix and its medium, inside the membrane, are mainly weak Van der Waals interactions between the side chains of the peptide and the hydrocarbon chains of the lipids. Thus, it is reasonable to assume that the proximity of the lipids do not alter strongly the flexibility of the peptide but only the time scale on which motions occur.

The hydrophobic environment of membrane raises the pK_a of Glu leading to protonated side chain able

to form hydrogen bond at physiological pH [19]. These arguments lead us to perform our calculations with Glu^9 in the protonated state.

The analysis of the correlations between the backbone dihedral angle fluctuations was undertaken to get a detailed picture of the dynamical behavior of both transmembrane helices. This study evidences a relationship between residues of the wild sequence for which conformational transitions or high dihedral angle fluctuations were previously observed [5]. We have found concerted motions between dihedral fluctuations of residues Leu^{13}, Val^{14}, Val^{15}, Val^{16} and Leu^{17}, located in the central part of the helix. In addition, another major characteristic of the wild transmembrane sequence is the lack of correlation between Ψ_8 and Φ_9 fluctuations. These two dihedral angles link residues Val^8 and Val^9 and define the local structure at the specific site for the mutation of the proto-oncogene encoded protein. A consequence of this lack of correlation is the induction of two negative correlations between distant residues, namely between Val^8 and Val^{16} and between Val^{16} and Ile^{23} which means that Val^{16} moves in opposite directions both with Val^8 and Ile^{23}. We note that high rms deviations due to transitions were found for the Φ dihedral angles of residues Val^8 and Val^{16}. Residue Val^8 is sequentially linked to Val^9 and is spatially close to Val^{16}, at two helix turns along the same face of the helix. Furthermore, Val^{16} is also at two helix turns of Ile^{23}. Local change at residues Val^8 and Val^9 induces the helical structure to be readjusted by the path Val^9–Val^{16}–Ile^{23}.

None of these effects reported for the transmembrane domain of the proto-oncogenic form of $p185^{c\text{-}erbB2}$ is observed for the corresponding domain of the oncogenic form. The classical anti-correlation network between adjacent dihedral angles in helical structure [20] is totally reproduced in the mutated sequence. The only concerted motion involving non-adjacent angles concerns a weak anti-correlation between Φ_9 and Ψ_{10} fluctuations.

The same protocol for the simulations of both peptides have been carried out to produce the trajectories. Thereby, this major different behavior originates certainly from the single residue replacement between the two sequences of the transmembrane domain.

The second part of this work was devoted to the propagation of a conformational perturbation along both transmembrane sequences. For the wild type sequence, the time dependence of correlation coefficients shows that in most cases the correlations between angular fluctuations of the backbone are amplified after a delay of a few picoseconds (Fig. 3). This observation suggests a propagation phenomenon along the helix, preceding a decay of the correlation. On the contrary, the correlation coefficients are not time dependent in the case of the oncogenic sequence and this result does not favour a propagation process.

The propagation phenomenon is also investigated by studying the response of a helix to an external disturbance at the N-terminus. We choose to introduce a deformation at residue Ile^4 by constraining Ψ_4 to 90°.

The average in formula (3) is an ensemble average because the system is in a non-equilibrium state. This is different from the conditions corresponding to formulas (1) and (2) in which the system is at the equilibrium, so that the ergodic principle allows to carry on time averages. Performing ensemble averages is very time and memory consuming because initial conditions for positions and velocities have to be sampled. In the present work, we have only used a small sampling of the initial velocities, so that no quantitative values can be expected from the present results, such as propagation velocity or mean deviations amplitude. Nevertheless, the results show without ambiguity that for the wild type peptide the perturbation is propagated and takes place progressively along the intramembrane sequence affecting first the residues close to the perturbation site and then the following residues. The effect of the perturbation consists of important fluctuations of the difference between dihedral angles of the perturbed (Ψ_4-constrained) and the unperturbed helices.

However, on the 2 ps time scale, both structures remain similar on the average and thus the effect of the initial perturbation on the other residues seems to be a dynamical process rather than a structural process. Of course, it can be envisaged that, on longer time scale, a conformational change is induced.

On the contrary, the mutated peptide is only locally disturbed as shown by the very weak effect beyond residue Gly^{10}. The apparent lack of propagation of the disturbance is certainly related to the

absence of correlation between dihedral angle fluctuations of non-adjacent residues.

All the results presented here strongly suggest that the wild transmembrane sequence of the c-*erb*B2 protein is much more flexible than that of its V659E mutant. It is worth noting that this conclusion is drawn from both long time and short time MD simulations which correspond to independent numerical experiments.

This study, within the limits of the model, leads to interesting suggestions for signal transmission process. The particular dynamics of the wild transmembrane spanning sequence originating from two regions far apart in the sequence, raises the question whether this dynamical behavior may have a role in transmembrane signalling. To explain this phenomenon, the existence of several active or inactive conformational states has been proposed [6]. From this hypothesis, it seems conceivable that motions in helices favour transitions from one inactive form to an other active form, with low cost in energy, in order to initiate the dimerization or oligomerization process necessary for kinase activity of the protein. This has been mentioned by Falke and Koshland [21] to explain the dimerization of the aspartate receptor. Also, the conformational change induced by ligand fixation at the extracellular part of the protein must be necessarily propagated along the sequence to induce other changes both in the structure and in the dynamics of the intramembrane sequence.

We have shown explicitly in this study that the propagation process can exist. This phenomenon may be the result from correlated motions between residues far apart in the sequence as observed in the particular case of the wild type transmembrane sequence of the c-*erb*B2 protein. Also, we have shown that a point mutation may dramatically alter the dynamical behavior of the transmembrane domain and that the replacement of Val^{659} by Glu^{659} abolishes concerted and propagated motions. A major consequence could be an equilibrium shift between the active and inactive forms.

Of course both biological and theoretical additional studies on other mutants should be necessary before to clearly establish a relationship between the dynamical and structural behavior of transmembrane domains of tyrosine kinase proteins and their biological activity.

Acknowledgements

We thank the Région Centre for supporting this work and the CITU from University of Orléans for computational facilities.

References

[1] M. Karplus and G.A. Petsko, Nature, 347 (1990) 631–639.
[2] J.A. MacCammon, Rep. Prog. Phys., 47 (1984) 1–46.
[3] J.A. MacCammon, B.R. Gelin and M. Karplus, Nature, 267 (1977) 585–590.
[4] S. Swaminathan, T. Ichiye, W.F. van Gunsteren and M. Karplus, Biochemistry, 21 (1982) 5230–5241.
[5] N. Garnier, D. Genest, E. Hebert and M. Genest, J. Biomol. Struct. Dyn., 11 (1994) 983–1002.
[6] A. Ullrich and J. Schlessinger, Cell, 61 (1990) 203–212.
[7] T. Yamamoto, S. Ikawa, T. Akiyama, K. Semba, N. Nomura, N. Miyajima, T. Saito and K. Toyoshima, Nature, 319 (1986) 230–234.
[8] J.G. Koland and R.A. Cerione, J. Mol. Biol., 263 (1988) 2230–2237.
[9] C. Greenfield, I. Hiles, M.D. Waterfield, M. Federwisch, A. Wollmer, T.L. Blundell and N. McDonald, EMBO J., 13 (1989) 4115–4123.
[10] R. Kubo, M. Toda and N. Hashitsume, Statistical Physics II, Springer-Verlag, Berlin, 1991.
[11] J.P. Ryckaert, G. Ciccotti and H.J.C. Berendsen, J. Comput. Phys., 23 (1977) 327–341.
[12] W.F. van Gunsteren and H.J.C. Berendsen, Mol. Phys., 34 (1977) 1311–1327.
[13] W.F. van Gunsteren and H.J.C. Berendsen, GROMOS Program System, Biomos Biomolecular Software, University of Groningen, 1987.
[14] J.A. MacCammon and S.C. Harvey, Dynamics of Proteins and Nucleic Acids, Cambridge University Press, Cambridge, 1987.
[15] C.L. Brooks III, M. Karplus and B.M. Petitt, Proteins: A Theoretical Perspective of Dynamics, Structure and Thermodynamics, Wiley, New York, 1988.
[16] S. Swaminathan, W.E. Jr. Harte and D.L. Beveridge, J. Am. Chem. Soc., 113 (1991) 2717–2721.
[17] T. Ichiye and M. Karplus, Protein: Struct. Function Genet., 11 (1991) 205–217.
[18] J.N. Israelachvili, S. Marcelja and R.G. Horn, Q. Rev. Biophys., 13 (1980) 121.
[19] M.J.E. Stemberg and W.J. Gullick, Protein Eng., 3 (1990) 245–248.
[20] R.M. Levy and M. Karplus, Biopolymers, 18 (1979) 2465–2495.
[21] J.J. Falke and D.E. Koshland, Science, 237 (1987) 1596–1600.